J Electr Eng Technol.2018; 13(2): 648-658
http://doi.org/10.5370/JEET.2018.13.2.648

ISSN(Print) 1975-0102
ISSN(Online) 2093-7423

MPC-based Two-stage Rolling Power Dispatch Approach for Wind-integrated Power System

Junyi Zhai*, Ming Zhou†, Shengxiao Dong*, Gengyin Li* and Jianwen Ren*

Abstract – Regarding the fact that wind power forecast accuracy is gradually improved as time is approaching, this paper proposes a two-stage rolling dispatch approach based on model predictive control (MPC), which contains an intra-day rolling optimal scheme and a real-time rolling base point tracing scheme. The scheduled output of the intra-day rolling scheme is set as the reference output, and the real-time rolling scheme is based on MPC which includes the leading rolling optimization and lagging feedback correction strategy. On the basis of the latest measured thermal unit output feedback, the closed-loop optimization is formed to correct the power deviation timely, making the unit output smoother, thus reducing the costs of power adjustment and promoting wind power accommodation. We adopt chance constraint to describe forecasts uncertainty. Then for reflecting the increasing prediction precision as well as the power dispatcher's rising expected satisfaction degree with reliable system operation, we set the confidence level of reserve constraints at different timescales as the incremental vector. The expectation of up/down reserve shortage is proposed to assess the adequacy of the upward/downward reserve. The studies executed on the modified IEEE RTS system demonstrate the effectiveness of the proposed approach.

Keywords: Two stage rolling power dispatch, Model predictive control, Wind power accommodation, Expectation of reserve shortage

1. Introduction

Wind power generation is variable in nature due to the variability of wind speed. Grid integration of this variable power in increasing capacity raises concern about its impact on the economy and reliability of the power system operation. Owing to the stochastic fluctuation and weak controllability of wind power, high penetration of wind power makes the power system dispatch more complicated. To keep reliable operation of the system with the high wind power penetration, more regulation capacity, generally undertaken by thermal units, has to be reserved. In this regard, reliability and economy of the system operation are somewhat conflicting, so how to coordinate generation and reserve of thermal units in a large scale wind power integrated system is a challenge.

To accommodate more wind power, the effective prediction is a prerequisite to model wind power variability. However, it is well acknowledged that the prediction precision of wind power is far lower than load forecast, especially long-term forecast, which may result in unfeasible day-ahead dispatch scheme. So the rolling dispatch approach consisting of day-ahead unit commitment (UC) and the intra-day rolling dispatch, is an effective solution since wind power prediction accuracy improves with time. In order to better accommodate wind power, how to design the rolling dispatch strategy is the key issue for the wind-integrated power system.

The uncertainty of wind power is a major challenge in the power system dispatch and accurate forecast is hard to achieve. Stochastic programming and robust optimization have been the most popular methods to handle wind power uncertainty in the UC problem. Given the probability distribution of wind power, UC can be formulated as a stochastic programming problem [1, 2]. The Gaussian distribution is also eligible to describe wind power forecast errors [3, 4]. For the security-constrained unit commitment (SCUC), multiple stochastic scenarios methods are proposed to describe the intermittency and volatility of wind power in Refs. [5]. Given the bounded uncertain dataset of various parameters, the optimal solution of robust optimization can satisfy all the constraints from this dataset, and it requires less knowledge about the uncertainty parameters [6].

Moreover, due to the uncertainty and weak controllability of wind power, the traditional reserve determination method, that is to take a certain percentage of load or the biggest committed unit's capacity [7], is no longer suitable. In Refs. [8], a hierarchical UC is presented to dispatch generation reserve, ramping reserve and transmission reserve, where normal and emergent operations are considered, and wind power is divided into two intervals based on confidence level, each interval is corresponding to different dispatch

† Corresponding Author: State Key Laboratory for Alternate Electrical Power System with Renewable Energy Sources, North China Electric Power University, Beijing, China. (zhouming@ncepu.edu.cn)
* State Key Laboratory for Alternate Electrical Power System with Renewable Energy Sources, North China Electric Power University, Beijing, China. (junyiwise@gmail.com)
Received: June 7, 2017; Accepted: December 22, 2017

strategies. In Refs. [9], the selection of spinning and non-spinning reserves is discussed through a market-clearing model. These researches are limited to a particular timescale; therefore the impact of wind power uncertainty on power dispatch at multi-time scales are not adequately addressed.

The average wind power forecast error is approximately 10% for the hour-ahead forecast, 15% for the 12-hour-ahead forecast, and even higher for a longer leading time [10]. Hence, it is essential to make rolling power dispatch schemes. In Refs. [11], the slow-response generation is scheduled at hourly timescale, while fast-response generation resources, including wind power, are scheduled at a sub-hour timescale. A rolling decision-making process is proposed in Refs. [12], where generation and reserve are co-optimized to minimize expected short-run operating cost. Based on the rolling coordination approach, a multi-temporal scale rolling-coordinated economic dispatch (ED) is presented in Refs. [13], to reduce the impact of ultra-short-term forecast errors on UC. Bao *et al* [14] established a day-ahead scheduling and real-time dispatch model to follow the uncertainty of renewable energy in microgrid. These power dispatch models mentioned above have employed a technique by refining the timescales to gradually accommodate wind power uncertainty, which is based on the characteristics that prediction precision is rising as the forecast horizon shortens.

Model predictive control (MPC) is a model-based finite-time closed-loop control method that has been widely used in the process industries. Compared to the open-loop optimal algorithm, MPC has stronger robustness, which is very suitable to deal with significant uncertainty. In Refs. [15] the application of nonlinear MPC in industry control process is performed. In Refs. [16], the MPC-based dynamic scheduling problem has been solved, verifying its better robustness in dealing with disturbance and uncertainties. Voltage regulation control strategy is analyzed in Refs. [17] where the traditional static voltage control strategy is replaced by the MPC-based optimization strategy. In Refs. [18], the MPC-based energy management system of distribution network with distributed generation is studied. In Refs. [19], MPC is introduced into the active power dispatch and control. Combined with the hierarchical control theory of large system, the hierarchical MPC method was proposed in Refs. [20] to optimize active power flow of wind power integrated power system. Till now, to the authors' knowledge, there is no research on MPC for the SCUC problem of wind power integrated power system.

The contributions of this paper are summarized as follows.

(1) MPC-based two-stage rolling power dispatch model is proposed which contains an intra-day rolling optimal scheme and a real-time rolling base point tracing scheme. The intra-day rolling scheme relies on the traditional open-loop optimal control algorithm to provide the thermal unit reference output for the real-time rolling scheme. Different from the traditional static real-time dispatch approach for a single time period, this real-time rolling base point tracing scheme is based on MPC which includes the leading rolling optimization and lagging feedback correction strategy to pursue the optimal performance in a future time window. On the basis of the latest measured thermal unit output feedback, the closed-loop optimization is formed to correct the power deviation timely, making the unit output smoother and reducing the costs of power adjustment. Therefore, multi-level coordination, gradual refinement and feedback correction can be brought together to deal with wind power fluctuation.

(2) Based on the occurrence probabilities of different power shortage, two indicators (EURS and EDRS) are proposed to assess the adequacy of upward and downward reserve. And the confidence level of reserve constraints at different timescales is set as the incremental vector to reflect the rising prediction precision and dispatcher's ever-rising expected satisfaction degree with the reliable system operation.

2. Two-stage Rolling Optimization Framework

2.1 Model assumptions

This MPC-based two-stage rolling power dispatch approach is based on the following assumptions.

(1) On-off states of the slow response thermal units have been scheduled in the day-ahead UC. This paper only focuses on the intra-day and real-time power dispatch schemes.

(2) The latest measured thermal unit output information is introduced to the MPC-based real-time rolling scheduling stage. It should be pointed out that it is feasible to collect the latest measured thermal unit output data and upload it to the power dispatch center.

(3) The forecast errors of load and wind power at different forecasting horizons are assumed to follow Gaussian distribution with zero mean and heteroscedasticity.

2.2 Rolling power dispatch framework

In this paper, the day-ahead and two-stage rolling power dispatch decisions are taken in an integrated manner. This means that the day-ahead schedule takes into account its effects on the two-stage rolling power dispatch decisions, and the latter should be consistent with the day-ahead schedule.

In the proposed two-stage rolling dispatch framework, the intra-day rolling optimal scheme is based on the traditional open-loop optimal control algorithm which is rolled every 15min, and the future 4hs' (16 periods in total) scheduling instructions are given. In this scheme, the on-off states of fast response units are scheduled to cope with the unexpected power deviation which is not covered in day-ahead UC. This scheme aims to provide the thermal unit reference output for the real-time rolling base point tracking scheme. The real-time rolling scheme is based on MPC which includes the leading rolling optimization and lagging feedback correction strategy to pursue the optimal performance in a future time window. The latest measured thermal units' output data is collected by the measurement system as an input to this scheme. This scheme is rolled every 5min, and the future 15mins' (3 periods in total) scheduling instructions are also given, but only the first period's scheduling instruction is implemented. The dispatch framework and optimization sequence diagram are presented in Fig. 1 and Fig. 2.

We assume that load and wind power uncertainties only influence the reserve demand, which means thermal unit output can be scheduled according to certain forecasts at different timescales, and the reserve capacity is scheduled to balance the uncertain forecast errors. The uncertainty variables are only included in the reserve constraints, and the feasible probability of reserve constraint is represented by confidence level.

In general, the closer to the operating time, the higher robustness of scheduling is required, and the longer to the operating time, the higher economy of scheduling is required. Hence, with the dispatch time approaches, the confidence level is rising to reflect the ever-rising characteristics of forecast accuracies and expected satisfaction degree with the reliable system operation. Reserve constraints can be properly loosened to avoid power overshooting at the long timescale, while be tightened to reduce the power adjustments at the short timescale. The economy and reliability of holistic dispatch are coordinated by the changes of different confidence level; as a result the forecast deviations are gradually accommodated.

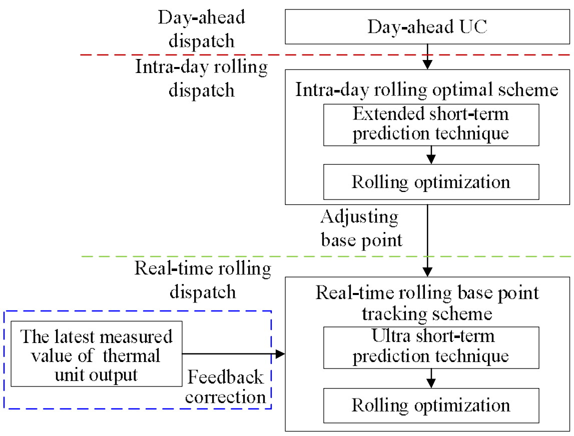

Fig. 1. Two-stage rolling power dispatch framework

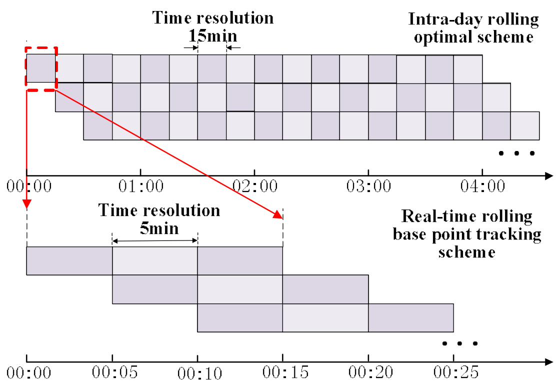

Fig. 2. Sequence diagram of the two-stage rolling power dispatch approach

2.3 Modeling load and wind power uncertainties

Since that load and wind power uncertainties modeling is required in our model, the uncertainty model is presented here. Load and wind power are expressed as the sum of the certain forecasts and the uncertain forecast errors, respectively. The load and wind power are modeled as below.

$$\begin{cases} D^{a}(t)=D^{f}(t)+\varepsilon_{D}(t) \\ P_{W}^{a}(t)=P_{W}^{f}(t)+\varepsilon_{W}(t) \end{cases} \tag{1}$$

where $D^{a}(t)$ and $P_{W}^{a}(t)$ are the actual values of load and wind power at time t, $D^{f}(t)$ and $P_{W}^{f}(t)$ are the forecasts of load and wind output at time t, $\varepsilon_{D}(t)$ and $\varepsilon_{W}(t)$ are the forecast errors of load and wind output at time t. As is mentioned above, $\varepsilon_{D}(t)\sim N(0,\sigma_{D}(t))$, $\varepsilon_{W}(t)\sim N(0,\sigma_{W}(t))$. The sum of $\varepsilon_{D}(t)$ and $\varepsilon_{W}(t)$ also follows Gaussian distribution, that is, $\varepsilon(t)\sim N(0,\sigma(t)^2)$, $\sigma(t)^2=\sigma_{D}(t)^2+\sigma_{W}(t)^2$.

2.4 The intra-day rolling optimal scheme

The intra-day rolling optimal scheme is based on the traditional open-loop optimal control algorithm, which is to provide the thermal unit reference output for the real-time rolling base point tracking scheme. Based on the fact that the on-off states of slow response thermal units have been determined by the day-ahead UC, only fast response thermal units' on-off states are scheduled in the intra-day scheme to cope with the unexpected power deviation. Since the extended short-term wind power forecast errors are relatively large, the confidence level to the reserve constraint of intra-day rolling scheme is set at a smaller value.

The intra-day rolling optimal scheme is modeled as follows:

$$\min F^{A}=\sum_{t=t_0+1}^{t_0+T^{A}}\sum_{i\in N_{G}}\left\{[a_i P_{Gi}(t)^2+b_i P_{Gi}(t)+u_i(t)c_i]+v_i(t)\rho_i^{SU}\right\} + \sum_{t=t_0+1}^{t_0+T^{A}}\sum_{j\in N_{W}}\rho_{cW}\Delta P_{Wj}^{A}(t) \tag{2}$$

$$s.t.\ \sum_{i\in N_G} P_{Gi}(t)+\sum_{j\in N_W}[P_{Wj}^{A}(t)-\Delta P_{Wj}^{A}(t)]=\sum_{d\in N_D} D_{d}^{A}(t) \tag{3}$$

$$\begin{cases}\Pr\{\sum_{i\in N_{\mathrm{G}}} R_{\mathrm{U}i}^{\mathrm{A}}(t)-\sum_{j\in N_{\mathrm{W}}}\Delta P_{\mathrm{W}j}^{\mathrm{A}}(t)\geq\varepsilon^{\mathrm{A}}(t)\}\geq\alpha^{\mathrm{A}}\\ R_{\mathrm{U}i}^{\mathrm{A}}(t)=\min[\overline{P}_{\mathrm{G}i}-P_{\mathrm{G}i}(t),RU_i]u_i(t)\end{cases} \tag{4}$$

$$\begin{cases}\Pr\{\sum_{i\in N_{\mathrm{G}}} R_{\mathrm{D}i}^{\mathrm{A}}(t)+\sum_{j\in N_{\mathrm{W}}}\Delta P_{\mathrm{W}j}^{\mathrm{A}}(t)\geq\varepsilon^{\mathrm{A}}(t)\}\geq\alpha^{\mathrm{A}}\\ R_{\mathrm{D}i}^{\mathrm{A}}(t)=\min[P_{\mathrm{G}i}(t)-\underline{P}_{\mathrm{G}i},RD_i]u_i(t)\end{cases} \tag{5}$$

$$u_i(t)\underline{P}_{\mathrm{G}i}\leq P_{\mathrm{G}i}(t)\leq u_i(t)\overline{P}_{\mathrm{G}i} \tag{6}$$

$$-u_i(t)RD_i\leq P_{\mathrm{G}i}(t)-P_{\mathrm{G}i}(t-1)\leq u_i(t-1)RU_i \tag{7}$$

$$\begin{cases}[T_i^{\mathrm{on}}(t-1)-\underline{T}_i^{\mathrm{on}}][u_i(t-1)-u_i(t)]\geq 0\\ [T_i^{\mathrm{off}}(t-1)-\underline{T}_i^{\mathrm{off}}][u_i(t)-u_i(t-1)]\geq 0\end{cases} \tag{8}$$

$$\begin{cases}v_i(t)-w_i(t)=u_i(t)-u_i(t-1)\\ v_i(t)+w_i(t)\leq 1\end{cases} \tag{9}$$

$$\left|\sum_{j\in N_{\mathrm{W}}} H_{\mathrm{W}j,l}[P_{\mathrm{W}j}^{\mathrm{A}}(t)-\Delta P_{\mathrm{W}j}^{\mathrm{A}}(t)]+\sum_{i\in N_{\mathrm{G}}} H_{\mathrm{G}i,l}P_{\mathrm{G}i}(t)-\sum_{d\in N_{\mathrm{D}}} H_{\mathrm{D}d,l}D_d^{\mathrm{A}}(t)\right|\leq\overline{L}_l \tag{10}$$

$$v_i(t)\in\{0,1\},\ w_i(t)\in\{0,1\},\ u_i(t)\in\{0,1\},\ \forall l\in L$$

where t_0 is the starting time of this scheme, $u_i(t)$ represents the on-off states of two types of thermal units, one is the on-off states of slow response thermal units which have already been determined by the day-ahead UC, and the other is the on-off states of fast response thermal units which are to be decided in this intra-day rolling scheme.

In the above formulation, the objective function (2) is to minimize the operating cost. Eq. (3) is the load balance constraint. Constraint (4) and (5) are the reserve chance constraints, (6) is the unit output limit, (7) is the ramp-up/-down rates limit, (8) is the minimum up/down time limit, (9) is the on-off states limit, (10) is the network security limit.

2.5 The real-time rolling base point tracking scheme

The real-time rolling base point tracking scheme is modeled based on MPC. MPC is a model-based finite-time closed-loop optimal control algorithm. MPC relies on dynamic models of the process, most often linear empirical models obtained by system identification. The main advantage of MPC is that it allows the current timeslot to be optimized while taking future timeslots into account. This is achieved by optimizing a finite time-horizon, but only implementing the current timeslot. MPC has the ability to anticipate future events and then take control actions accordingly.

The latest thermal units' output data is collected by the measurement system as an input to this scheme. The multi-step dynamic rolling optimization and feedback correction strategy are adopted to cover the power deviation timely. At each sampling time, the future 15mins' (3 periods in total) thermal unit output increments are calculated based on the unit output model. When the power deviation occurs, the control mode with the smallest power adjustments is adopted to ensure the economy, but only the first period's output increment will be implemented. Compared with the traditional static real-time dispatch approach for a single time period, this real-time rolling scheme has stronger robustness.

2.5.1 Unit output model

The ultra short-term wind power forecasts are taken as the input variables, the latest measured value of thermal unit output is taken as initial values and the future 15mins' (T^{B} periods in total, $T^{\mathrm{B}}=3$) thermal unit output increments are made as control variables, that is:

$$P_{\mathrm{G}i}(t+k\,|\,t)=P_{\mathrm{G}i}^{\mathrm{ini}}(t)+\sum_{\tau=1}^{k}\Delta P_{\mathrm{G}i}(t+\tau\,|\,t),k=1,2,...,T^{\mathrm{B}} \tag{11}$$

where t is the current sampling time, $\Delta P_{\mathrm{G}i}(t+\tau\,|\,t)$ is the output increments of unit i at future period $(t+(\tau-1),t+\tau]$ which is to be optimized at current sampling time t, and it is set as the control variable in MPC, $P_{\mathrm{G}i}(t+k\,|\,t)$ denotes the output of thermal unit i at future time $t+k$ which is to be determined at current sampling time t, $P_{\mathrm{G}i}^{\mathrm{ini}}(t)$ is the initial output of thermal unit i, that is, the latest unit output collected by the measurement system at current sampling time t.

2.5.2 Rolling optimization

Since the real-time rolling scheme is close to the execution of actual dispatch, it is impossible to start up or shut down units. The unit commitment determined by intra-day rolling scheme is set as the reference. At this timescale, the prediction precision is high enough, and the dispatcher's requirement for reliability, which can also be regarded as the dispatcher's expected satisfaction degree with reserve constraints, is also at a higher level. Thus, the confidence level is set at a larger value to ensure operation reliability.

For the current sampling time t, the real-time rolling base point tracking scheme is modeled as follows:

$$\begin{aligned}\min F^{\mathrm{B}}(t)&=\sum_{k=1}^{T^{\mathrm{B}}}\sum_{i\in N_{\mathrm{G}}}\gamma\left|P_{\mathrm{G}i}(t+k\,|\,t)-\tilde{P}_{\mathrm{G}i}(t+k)\right|\\&+\sum_{k=1}^{T^{B}}\sum_{j\in N_{\mathrm{W}}}\rho_{\mathrm{cW}}\Delta P_{\mathrm{W}j}^{B}(t+k)\\&=\sum_{k=1}^{T^{\mathrm{B}}}\sum_{i\in N_{\mathrm{G}}}\gamma\left|P_{\mathrm{G}i}^{\mathrm{ini}}(t)+\sum_{t=1}^{k}\Delta P_{\mathrm{G}i}(t+\tau\,|\,t)-\tilde{P}_{\mathrm{G}i}(t+k)\right|\\&+\sum_{k=1}^{T^{B}}\sum_{j\in N_{\mathrm{W}}}\rho_{\mathrm{cW}}\Delta P_{\mathrm{W}j}^{B}(t+k)\end{aligned} \tag{12}$$

s.t.

$$\sum_{i\in N_{\mathrm{G}}}[P_{\mathrm{G}i}^{\mathrm{ini}}(t)+\sum_{\tau=1}^{k}\Delta P_{\mathrm{G}i}(t+\tau\,|\,t)]+\sum_{j\in N_{\mathrm{W}}}[P_{\mathrm{W}j}^{\mathrm{B}}(t+k)-\Delta P_{\mathrm{W}j}^{\mathrm{B}}(t+k)] = \sum_{d\in N_{\mathrm{D}}} D_d^{\mathrm{B}}(t+k) \tag{13}$$

$$\begin{cases}\Pr\{\sum_{i\in N_{\mathrm{G}}} R_{\mathrm{U}i}^{\mathrm{B}}(t+k)-\sum_{j\in N_{\mathrm{W}}}\Delta P_{\mathrm{W}j}^{\mathrm{B}}(t+k)\ge \varepsilon^{\mathrm{B}}(t+k)\}\ge \alpha^{\mathrm{B}} \\ R_{\mathrm{U}i}^{\mathrm{B}}(t+k)=\min[\overline{P}_{\mathrm{G}i}-P_{\mathrm{G}i}^{\mathrm{ini}}(t)-\sum_{\tau=1}^{k}\Delta P_{\mathrm{G}i}(t+\tau\,|\,t),RU_i/3]\end{cases} \tag{14}$$

$$\begin{cases}\Pr\{\sum_{i\in N_{\mathrm{G}}} R_{\mathrm{D}i}^{\mathrm{B}}(t+k)+\sum_{j\in N_{\mathrm{W}}}\Delta P_{\mathrm{W}j}^{\mathrm{B}}(t+k)\ge \varepsilon^{\mathrm{B}}(t+k)\}\ge \alpha^{\mathrm{B}} \\ R_{\mathrm{D}i}^{\mathrm{B}}(t+k)=\min[P_{\mathrm{G}i}^{\mathrm{ini}}(t)+\sum_{\tau=1}^{k}\Delta P_{\mathrm{G}i}(t+\tau\,|\,t)-\underline{P}_{\mathrm{G}i,t},RD_i/3]\end{cases} \tag{15}$$

$$\underline{P}_{\mathrm{G}i}\le P_{\mathrm{G}i}^{\mathrm{ini}}(t)+\sum_{\tau=1}^{k}\Delta P_{\mathrm{G}i}(t+\tau\,|\,t)\le \overline{P}_{\mathrm{G}i} \tag{16}$$

$$-RD_i/3\le\sum_{\tau=1}^{k}\Delta P_{\mathrm{G}i}(t+\tau\,|\,t)-\sum_{\tau=1}^{k-1}\Delta P_{\mathrm{G}i}(t+\tau\,|\,t)\le RU_i/3 \tag{17}$$

$$\left|\sum_{i\in N_{\mathrm{G}}} H_{\mathrm{G}i,l}[P_{\mathrm{G}i}^{\mathrm{ini}}(t)+\sum_{\tau=1}^{k}\Delta P_{\mathrm{G}i}(t+\tau\,|\,t)]-\sum_{d\in N_{\mathrm{D}}} H_{\mathrm{D}d,l}D_d^{\mathrm{B}}(t)(t+k) + \sum_{j\in N_{\mathrm{W}}} H_{\mathrm{W}j,l}[P_{\mathrm{W}j}^{\mathrm{B}}(t+k)-\Delta P_{\mathrm{W}j}^{\mathrm{B}}(t+k)]\right|\le \overline{L}_l \tag{18}$$

where $\tilde{P}_{\mathrm{G}i}(t+k)$ is the reference output of thermal unit i at future time $t+k$ determined by the intra-day rolling scheme.

In the above formulation, the objective function (12) is to minimize the power deviations. Constraints (13)-(18) are similar to (3)-(7) and (10).

When the output increments in the future 15min(3 periods in total) are solved at current sampling time t, only the first period's output increment $\Delta P_{\mathrm{G}i}(t+1\,|\,t)$ is implemented and then the planned thermal unit output of the next moment t+1 is updated:

$$P_{\mathrm{G}i}(t+1\,|\,t)=P_{\mathrm{G}i}^{\mathrm{ini}}(t)+\Delta P_{\mathrm{G}i}(t+1\,|\,t) \tag{19}$$

2.5.3 Feedback correction

The above rolling optimization is a leading control based on forecasts. However, at the present wind power prediction accuracy, the advanced control can cause power deviation between the actual output and the planned output of thermal unit. Therefore, the lagging feedback correction strategy is introduced. At each sampling time, the latest measured thermal unit output is adopted to correct the unit output determined by the rolling optimization strategy. Thus, the closed-loop optimization is formed to cover the power deviation timely and make the future time's thermal unit output closer to the reality.

For the next sampling moment t+1, a new round rolling optimization will be carried out, and the latest measured thermal unit output of time t+1 is set as the initial value. That is:

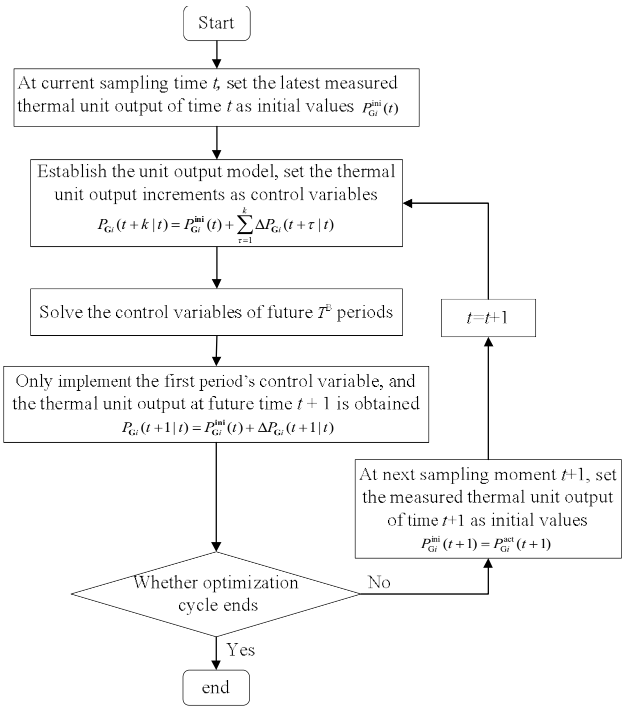

Fig. 3. Flow chart of the real-time rolling base point tracking scheme

$$P_{\mathrm{G}i}^{\mathrm{ini}}(t+1)=P_{\mathrm{G}i}^{\mathrm{act}}(t+1) \tag{20}$$

where $P_{\mathrm{G}i}^{\mathrm{act}}(t+1)$ represents the measured output of thermal unit i at the next sampling moment t+1 which is collected by the measurement system.

The optimization flow chart of the real-time rolling base point tracking scheme is shown in Fig. 3.

3. Assessment of Reserve Adequacy Considering Uncertainties

The significant volatility of wind power puts forward higher requirement to the reserve capacity, so we propose two indicators: up and down reserve shortage expectation, to quantify the system reserve level, as well as reflect the adequacy of the upward reserve and the downward reserve.

The Cauchy, Beta or Gaussian distributions are the widely-used techniques to model the uncertainty in power systems. As for many geographically dispersed wind farms, according to the central limit theorem, the forecast error is usually assumed as a random variable that obeys the law of Gaussian distribution. In [3, 4], the Gaussian distribution has been widely applied to approximate the probability density function of the wind power generation. For the sake of simplicity, the load and wind power forecast errors at different forecasting horizons are assumed to

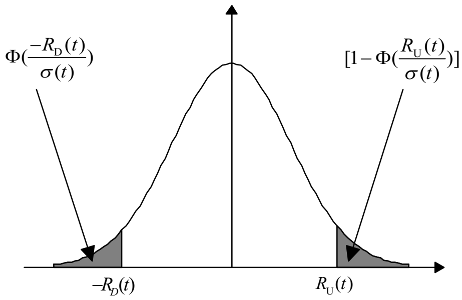

Fig. 4. Interval distribution of EURS and EDRS

follow Gaussian distribution with zero mean and heteroscedasticity in this paper. Based on this assumption, the interval distribution of the expectation of up reserve shortage (EURS) and the expectation of down reserve shortage (EDRS) are shown in Fig. 4. The gray area at right side is defined as the EURS, and the gray area at left side is defined as the EDRS. The EURS (EDRS) stands for the up (down) reserve deficiency, that is, when the sum of actual load and wind power is less (greater) than the forecasts, the up (down) reserve capacity will be less than the quantity of power fluctuation.

Based on the occurrence probabilities of different power shortages, indicators of EURS R_+ and EDRS R_- are proposed and deduced in (21) and (22) to reflect the adequacy of upward reserve and the downward reserve.

$$\begin{aligned} R_+(t) &= \int_{R_U(t)}^{+\infty} (x - R_U(t)) \frac{1}{\sqrt{2\pi}\sigma(t)} e^{\frac{-x^2}{2\sigma(t)^2}} dx \\ &= \frac{\sigma(t)}{\sqrt{2\pi}} e^{\frac{-R_U(t)^2}{2\sigma(t)^2}} - R_U(t)[1 - \Phi(\frac{R_U(t)}{\sigma(t)})] \end{aligned} \tag{21}$$

$$\begin{aligned} R_-(t) &= \int_{-\infty}^{-R_D(t)} (-R_D(t) - x) \frac{1}{\sqrt{2\pi}\sigma(t)} e^{\frac{-x^2}{2\sigma(t)^2}} dx \\ &= \frac{\sigma(t)}{\sqrt{2\pi}} e^{\frac{-R_D(t)^2}{2\sigma(t)^2}} - R_D(t)\Phi(\frac{-R_D(t)}{\sigma(t)}) \end{aligned} \tag{22}$$

where $\Phi(\cdot)$ represents the standard normal distribution function.

4. Deterministic Equivalents of the Reserve Constraints

Based on the assumption that load and wind power forecast errors follow Gaussian distribution, the chance constrained programming is applied to deal with uncertainty variables. This rolling power dispatch approach is cast as a two-stage stochastic programming problem, where the first stage deals with the SCUC problem in the intra-day rolling scheme, and the second stage represents the security-constrained economic dispatch(SCED) problem in the real-time rolling scheme.

For each rolling dispatch model, only the reserve constraints are chance constraints, and others are deterministic constraints. So the reserve constraints which contain random variables are transformed into deterministic equivalents at every timescale to reduce the model solution difficulty.

For the function $g(x,\xi) = \xi - h(x)$, if and only if $h(x) \ge K_\alpha = \phi^{-1}(\alpha)$, then $\Pr\{h(x) \ge \xi\} \ge \alpha$, the smallest one is chosen to be the solution of $\Pr\{h(x) \ge \xi\} \ge \alpha$, given by

$$K_\alpha = \inf\{K \mid K = \phi^{-1}(\alpha)\} \tag{23}$$

where $\phi(\cdot)$ is the probability distribution function of the random variables; $\phi^{-1}(\cdot)$ is the inverse function. Take the intra-day rolling scheme for example, the deterministic equivalent of the up reserve constraint is given by

$$\begin{aligned} &\sum_{i\in N_G} \min[\overline{P}_{Gi} - P_{Gi}(t), RU_i]u_i(t) - \sum_{j\in N_W} \Delta P_{Wj}^{A}(t) \ge K_{\alpha^A}(t) \\ &= \inf\{K \mid \int_{-\infty}^{K} \frac{1}{\sqrt{2\pi}\sigma(t)} e^{-\frac{x^2}{2\sigma(t)^2}} dx = \alpha^A\} \\ &= \inf\{K \mid K = \phi^{-1}(t, \alpha^A)\} \end{aligned} \tag{24}$$

The deterministic equivalent of the down reserve constraint is given by

$$\begin{aligned} &\sum_{i\in N_G} \min[P_{Gi}(t) - \underline{P}_{Gi}, RD_i]u_i(t) + \sum_{j\in N_W} \Delta P_{Wj}^{A}(t) \ge K_{\alpha^A}(t) \\ &\quad = \inf\{K \mid \int_{-\infty}^{K} \frac{1}{\sqrt{2\pi}\sigma(t)} e^{-\frac{x^2}{2\sigma(t)^2}} dx = \alpha^A\} \\ &\quad = \inf\{K \mid K = \phi^{-1}(t, \alpha^A)\} \end{aligned} \tag{25}$$

Now the reserve constraints have been transformed into deterministic equivalents, the proposed dispatch model is a mixed integer nonlinear programming problem at each stage. The mathematical programming software GUROBI is used to solve the two-stage rolling optimization model.

5. Numerical Simulations

5.1 Case data

The performance of MPC-based two-stage rolling dispatch approach is tested on the IEEE RTS system. Assuming that only the hot start of hermal unit is considered, thermal unit 1 and 2, 5 and 6 and 15 to 19 are fast response units and others are slow response units. The thermal unit data, line data and bus load proportion can be found in Refs. [21, 22]. A wind farm replaces six hydro units at bus 22. The load and wind power curves of 8h (96 time intervals in total) are shown in Fig. 5. The prediction

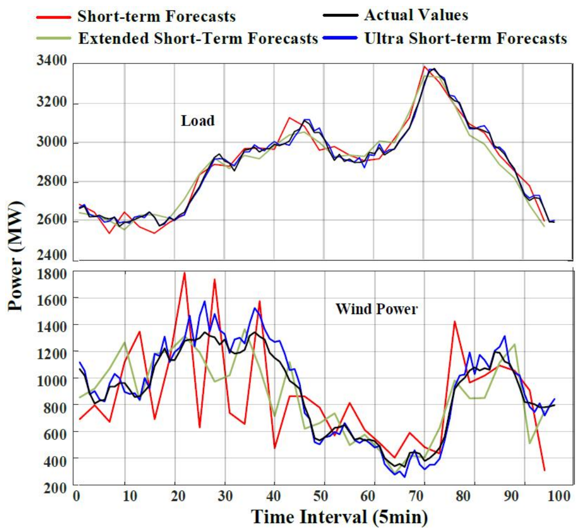

Fig. 5. Load and wind power curve

curves are obtained by adding disturbance to the actual power curves. Assuming the wind power short-term forecast error is 30%, then the day-ahead wind power forecasts are obtained based on the actual wind power with the addition of white noise whose expectation is 0 and the standard deviation is 0.3 times the forecasts. Similarly, assuming the extended short-term forecast error and ultra short-term forecast error of wind power are 15%, 10%, respectively, and the short-term forecast error, extended short-term forecast error and ultra short-term forecast error of load are 1.5%, 1%, 0.5%, respectively. The penalty cost of curtailed wind is 100\$/MW, the power adjustment cost is 10\$/MW, and the confidence level incremental vector of reserve constraints is set as $\vec{\boldsymbol{\alpha}}=[\alpha^{A},\alpha^{B}]=[0.9, 0.95]$.

5.2 Results analysis of two-stage rolling dispatch

Fig. 6 illustrates the output curves of thermal unit 8, unit 20, unit 22 and unit 24 given by our two-stage rolling power dispatch approach and day-ahead UC, indicating that the thermal unit output in the real-time rolling scheme is smoother. Fig. 7 presents the contrast curve of power deviation between the planned total generation output and the actual electricity demand in different dispatch schemes. For the day-ahead UC, the power deviation is enormous, which cannot satisfy the actual scheduling requirements. While in the intra-day rolling scheme, the planned total generation output is relatively close to the actual electricity demand, and the power deviation in the real-time rolling scheme is tiny, which can well match the actual load demand. We can conclude that the two-stage rolling power dispatch approach can gradually adjust the thermal unit output determined by the day-ahead UC, so as to ease the power adjustment burden and reduce the power adjustment costs.

Full accommodation of wind power is not a must in our rolling dispatch model. Instead, we attach importance to the satisfaction degree with down reserve constraints at the corresponding dispatch scheme and allow the occurrence of wind curtailment. The wind power curtailment amount and wind power curtailment rate at different dispatch schemes are shown in Fig. 8 and Table 1. The wind power curtailment rate of day-ahead UC is 17.2%. After the correction of two-stage rolling dispatch scheme, the wind power curtailment rate has dropped to 4.9%, indicating that the single day-ahead dispatch can cause severe wind power curtailment problem and the two-stage rolling dispatch scheme can effectively promote wind power accommodation. Thus, multi-level coordination, gradual refinement and feedback correction can be brought together to deal with wind power fluctuation.

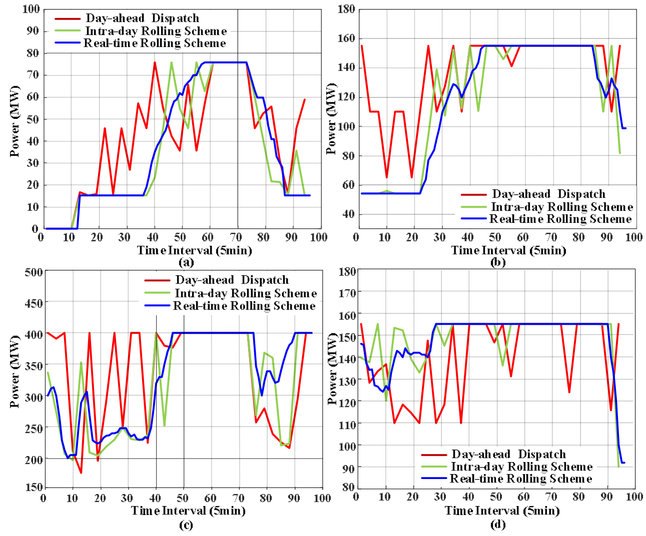

Fig. 6. Unit output curve of (a) unit 8, (b) unit 20, (c) unit 22, (d) unit 24

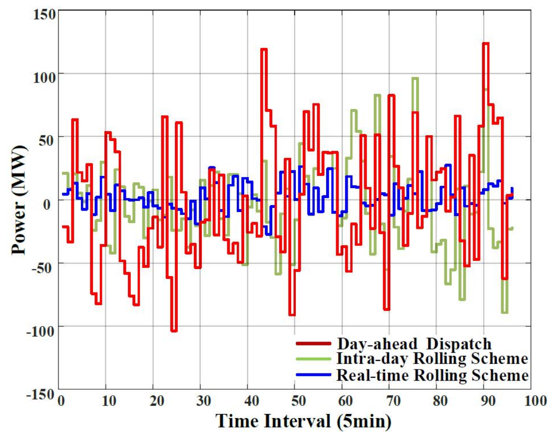

Fig. 7. Contrast curve of power deviation in different dispatch schemes

Besides, the EDRS at different dispatch schemes is shown in Fig. 9 to evaluate the adequacy of down reserve, indicating that the day-ahead dispatch has the greatest EDRS and the real-time rolling scheme has the smallest. With the dispatch time approaches, the wind power

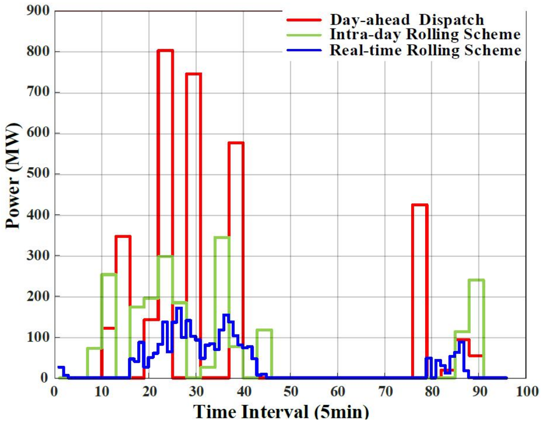

Fig. 8. Wind power curtailment amount at different dispatch schemes

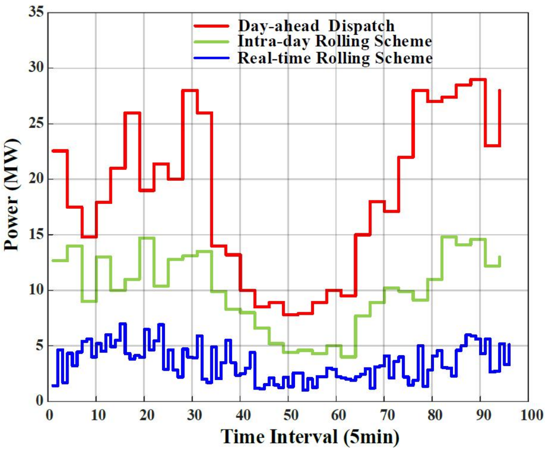

Fig. 9. Expectation of down reserve shortage (EDRS)

Table 1. Wind power curtailment rate at different dispatch schemes

	Day-ahead UC	Intra-day rolling optimal scheme	Real-time rolling base point tracing scheme
Wind power curtailment rate	17.2%	12.4%	4.9%

prediction precision and the confidence level of the down reserve constraints is rising, leading to the gradual decrease of EDRS. That is to say, the risk of the system down reserve shortage is gradually reducing, and the system operation reliability is improved progressively.

5.3 Comparisons of different dispatch approaches

To compare the output smoothness of thermal unit in the single day-ahead dispatch mode and the MPC-based two-stage rolling dispatch mode, the output variances of slow response thermal units are shown in Fig. 10, illustrating that the thermal unit output of the single day-ahead dispatch mode has higher variances than those of the MPC-based two-stage rolling dispatch mode. That is to say, the two-stage rolling dispatch approach can make the thermal unit output smoother to well accommodate the wind power fluctuation.

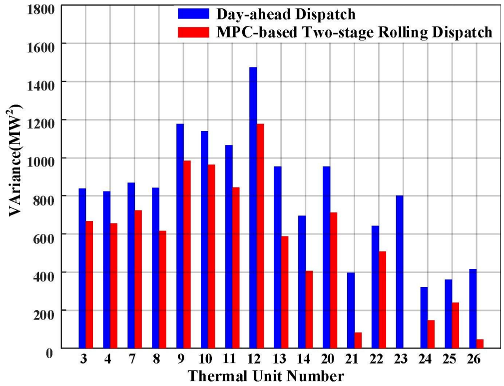

Fig. 10. Unit output variances of day-ahead dispatch mode and two-stage rolling dispatch mode

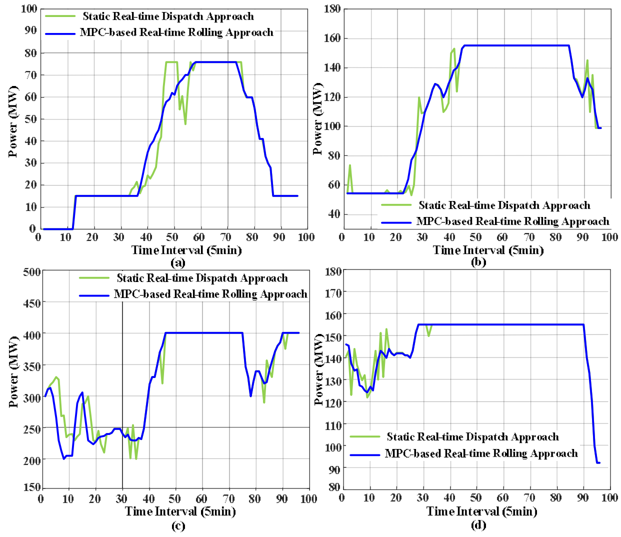

Fig. 11. Thermal unit output curve of two real-time dispatch approaches of (a) unit 8, (b) unit 20, (c) unit 22, (d) unit 24

On the basis of intra-day rolling optimal scheme, two real-time dispatch modes are adopted for comparison. Mode 1 is the proposed MPC-based real-time rolling base point tracking mode; mode 2 is the traditional static real-time dispatch approach for a single time period. The output curve of typical thermal units and the output variances of slow response thermal units in the dispatch cycle of these two real-time dispatch modes are shown in Fig. 11 and Fig. 12, illustrating that the thermal unit output in mode 1 is smoother than that of mode 2. As mode 1 has taken into account the forecasts in a future finite-time window and the influence of latest measured thermal unit output on the current dispatch status, it can avoid the repeated adjustment and over-regulation of thermal unit output, which is beneficial to accommodate the wind power fluctuation and can make the thermal unit output smother. Through two-

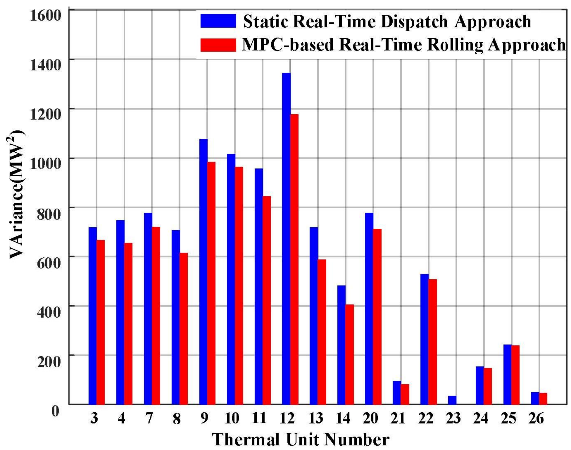

Fig. 12. Unit output variances of two real-time dispatch approaches

Table 2. Comparisons between two different real-time dispatch approaches

	MPC-based real-time rolling mode (mode 1)	Traditional static real-time dispatch mode (mode 2)
Wind power curtailment rate	4.9%	6.7%
Total costs of power adjustment ($)	62 902	77 224

stage rolling power dispatch, the system operation reliability can be improved, the mechanical loss of thermal unit can be reduced and the working life of thermal unit can be extended at the same time.

The total costs of power adjustment and the wind power curtailment rate of two real-time dispatch modes are compared in Table 2. Total output adjustment costs of Mode 1 is only 81% of model 2, while the wind power curtailment rate is reduced by 1.8%. We can conclude that mode 1 is more conducive to promoting wind power accommodation and reducing the costs of power adjustment in the real-time dispatch stage. Since mode 1 adopts the future 15min's thermal unit output increments as the control variables and continuously takes the latest measured thermal unit output to feedback to this scheme, the power deviation caused by stochastic factors can be timely correct, and the power adjustment costs can be reduced.

6. Conclusions

In this paper, we present a two-stage generation and reserve joint optimization approach based on MPC for wind power integrated power systems, which contain an intra-day rolling optimal scheme and a real-time rolling base point tracing scheme. The scheduling output of the long timescale scheme is set as the reference output, and the real-time rolling scheme is based on MPC to pursue the optimal performance in a future time window. Considering that wind power forecasts at different timescales have variable accuracies, we set the confidence level of reserve constraints at different timescales as the incremental vector to reflect the time-varying characteristics of forecast errors and the dispatcher's expectation to reliable operation. The expectation of up and down reserve shortage is therefore proposed to reflect the adequacy of the upward reserve and the downward reserve.

Simulations on the IEEE RTS system shows that the proposed MPC-based two-stage rolling dispatch approach can better adjust the reserve demand and the unit outputs according to the continuously updated forecasts, and the power fluctuations can be coordinated and accommodated gradually. Multi-level coordination, gradual refinement and feedback correction can be brought together to maximize wind power accommodation.

For a real system, although the optimization scale will become larger, the two-stage rolling scheme can significantly reduce the adjustment burden of AGC units. The situation that the AGC adjustment capability cannot deal with the large fluctuation of wind power in the real-time stage and the possible wind power curtailment or load shedding can be avoided. The future work is to study how to decouple and coordinate the time dimension and the space dimension of the real-time rolling model, so as to obtain a more practical model suitable for the online applications. This puts forward the requirements for the efficiency of real-time rolling algorithm and will be one of our future research areas.

Acknowledgments

The authors are grateful to the National Key Research and Development Program (2016YFB0900100) and the Fundamental Research Funds for the Central Universities (2018QN001).

Nomenclature

A. Indices and Sets

d	Index of load buses.
i	Index of thermal units.
j	Index of wind farms.
l	Index of load lines.
L	Set of internal lines.
N_{D}	Set of load buses.
N_{G}	Set of thermal units.
N_{W}	Set of wind farms.

B. Variables

$u_i(t)$	On-off states of thermal unit *i* at time *t*.
$v_i(t)/w_i(t)$	Start/stop actions of thermal unit *i* at time *t*.
$P_{\mathrm{G}i}(t)$	Output of thermal unit *i* at time *t*.

$R_{\mathrm{U}i}^{\mathrm{A}}(t) / R_{\mathrm{U}i}^{\mathrm{B}}(t)$ Available up reserve capacity of unit i at time t in the intra-day/real-time rolling scheme.
$R_{\mathrm{D}i}^{\mathrm{A}}(t) / R_{\mathrm{D}i}^{\mathrm{B}}(t)$ Available down reserve capacity of unit i at time t in the intra-day/real-time rolling scheme.
$\Delta P_{\mathrm{W}j}^{\mathrm{A}}(t)$ / $\Delta P_{\mathrm{W}j}^{\mathrm{B}}(t)$ Wind power curtailed amount of wind farm j at time t in the intra-day/real-time rolling scheme.

C. Parameters

a_i, b_i, c_i Fuel cost coefficients of thermal unit i.
ρ_i^{SU} Start-up cost of thermal unit i.
γ Power adjustment cost in the real-time rolling scheme.
ρ_{cW} Penalty price of curtailed wind power.
$\varepsilon^{\mathrm{A}}(t) / \varepsilon^{\mathrm{B}}(t)$ Sum of load and wind power forecast errors at time t in the intra-day/real-time rolling scheme.
$\alpha^{\mathrm{A}} / \alpha^{\mathrm{B}}$ Confidence level of the intra-day/real-time rolling scheme.
$D_d^{\mathrm{A}}(t) / D_d^{\mathrm{B}}(t)$ Load forecasts of bus d at time t in the intra-day/real-time rolling scheme.
$H_{\mathrm{G}i,l}$ / $H_{\mathrm{W}j,l}$ / $H_{\mathrm{D}d,l}$ Power transfer distribution factor of thermal unit i, wind farm j and load d.
$\overline{L}_l$ Maximum transmission power of line l.
$\underline{P}_{\mathrm{G}i} / \overline{P}_{\mathrm{G}i}$ Minimum/maximum power output of thermal unit i.
$P_{\mathrm{W}j}^{\mathrm{A}}(t) / P_{\mathrm{W}j}^{\mathrm{B}}(t)$ Power forecasts of wind farm j at time t in the intra-day/real-time rolling scheme.
RU_i / RD_i Ramp-up/-down limit of 15min of thermal unit i.
$R_{\mathrm{U}}(t) / R_{\mathrm{D}}(t)$ Available up/down reserve capacity at time t.
$T^{\mathrm{A}} / T^{\mathrm{B}}$ Time periods of the intra-day/real-time rolling scheme.
$T_i^{\mathrm{on}}(t-1)$ / $T_i^{\mathrm{off}}(t-1)$ Continuous starting up/off time of thermal unit i up to time t-1.
$\underline{T}_i^{\mathrm{on}} / \underline{T}_i^{\mathrm{off}}$ Minimum continuous starting up/off time of thermal unit i.

References

[1] P. Xiong and P. Jirutitijaroen, "A stochastic optimization formulation of unit commitment with reliability constraints," *IEEE Trans. Smart Grid*, vol. 4, no. 4, pp. 2200-2208, 2013.
[2] W. Cui, W. Yan, W. Lee, X. Zhao, Z. Ren and C. Wang, "A two-stage stochastic programming model for optimal reactive power dispatch with high penetration level of wind generation," *J Electr Eng Technol*, vol. 12, no. 1, pp. 53-63, 2017.
[3] H. Park, R. Baldick and D. P. Morton, "A stochastic transmission planning model with dependent load and wind forecasts," *IEEE Trans. Power Syst.*, vol. 30, no. 6, pp. 3003-3011, 2015.
[4] D. Huang, L. Xie and Z. Wu, "Dynamic economic dispatch for microgrid based on the chance-constrained programming," *J Electr Eng Technol*, vol. 12, no. 3, pp. 1064-1072, 2017.
[5] Sung-Eun Lee, Dong-Jun Won and Il-Yop Chung, "Operation scheme for a wind farm to mitigate output power variation," *J Electr Eng Technol*, vol. 7, no. 6, pp. 869-875, 2012.
[6] A. Lorca and X. A. Sun, "Adaptive robust optimization with dynamic uncertainty sets for multi-period economic dispatch under significant wind," *IEEE Trans. Power Syst.,* vol. 30, no. 4, pp. 1702-1713, 2015.
[7] C. Ngygen and H. Lee, "Optimization of wind power dispatch to minimize energy storage system capacity," *J Electr Eng Technol*, vol. 9, no. 3, pp. 1080-1088, 2014.
[8] B. Zhou, G. Geng and Q. Jiang, "Hierarchical unit commitment with uncertain wind power generation," *IEEE Trans. Power Syst.*, vol. 31, no. 1, pp. 94-104, 2016.
[9] J. M. Morales, A. J. Conejo and J. Pérez-Ruiz, "Economic valuation of reserves in power systems with high penetration of wind power," *IEEE Trans. Power Syst.*, vol. 24, no. 2, pp. 900-910, 2009.
[10] F. Li and Y. Wei, "A probability-driven multilayer framework for scheduling intermittent renewable energy," *IEEE Trans. Sustain. Energy*, vol. 3, no. 3, pp. 455-464, 2012.
[11] H. Gangammanavar, S. Sen and V. M. Zavala, "Stochastic optimization of sub-hourly economic dispatch with wind energy," *IEEE Trans. Power Syst.*, vol. 31, no. 2, pp. 949-959, 2016.
[12] J. Warrington, C. Hohl, P.J. Goulart, and M. Morari, "Rolling unit commitment and dispatch with multi-stage recourse policies for heterogeneous devices," *IEEE Trans. Power Syst.*, vol. 31, no. 1, pp. 187-197, 2016.
[13] K. Wang, B. Zhang, D. Yan, Y. Li and T. Luo, "A multi-time scale rolling coordination scheduling method for power grid integrated with large scale wind farm," *Power System Technology*, vol. 38, no. 9, pp. 2434-2440, 2014.
[14] Z. Bao, Q. Zhou, Z. Yang, Q. Yang, L. Xu and T. Wu, "A multi time-scale and multi energy-type coordinated microgrid scheduling solution-part i: model and methodology," *IEEE Trans. Power Syst.*, vol. 30, no. 5, pp. 2257-2266, 2015.
[15] E. Gallestey, A. Stothert, M. Antoine and S. Morton, "Model predictive control and the optimization of power plant load while considering life time consumption," *IEEE Trans. Power Syst.*, vol. 17, no. 5, pp. 186-191, 2002.
[16] X. Xia, J. Zhang and A. Elaiw, "A model predictive control approach to dynamic economic dispatch

problem," 2009 IEEE Bucharest Power Tech, 1-7, 2009.
[17] F. Xu, Q. Guo and H. Sun, "Automatic voltage control of wind farms based on model predictive control theory," *Automation of Electric Power System*, vol. 39, no. 7, pp. 59-67, 2015.
[18] M. Falahi, S. Lotfifard, M. Ehsani and K. Butler-Purry, "Dynamic model predictive- based energy management of DG integrated distribution systems," *IEEE Trans. Power Syst*., vol. 28, no. 4, pp. 2217-2226, 2013.
[19] L. Xie and M. D. Ilić, "Model predictive economic/ environmental dispatch of power systems with intermittent resources" IEEE Power & Energy Society General Meeting, Canada, 1-6, 2009.
[20] B. Zhang, J. Chen and W. Wu, "A hierarchical model predictive control method of active power for accommodating large-scale wind power integration," *Automation of Electric Power System*, vol. 38, no. 9, pp. 6-14, 2014.
[21] S. J. Wang, S. M. Shahidehpour, D. S. Kirschen, S. Mokhtari and G. D. Irisarri, "Short-term generation scheduling with transmission and environmental constraints using an augmented lagrangian relaxation," *IEEE Trans. Power Syst.*, vol. 10, no. 3, pp. 1294-1301, 1995.
[22] P. M. Subcommittee, "IEEE reliability test system," *IEEE Trans. Power App. Syst.*, PAS-98, 2047-2054, 1979.

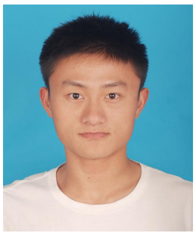

Junyi Zhai He received the B.S. degree in electrical engineering from North China Electricity Power University, Beijing, China, in 2014. His research interest is power system operation.

Ming Zhou She received the B.S., M.S., and Ph.D. degrees in electrical engineering from North China Electricity Power University, Beijing, China, in 1989, 1992, and 2006, respectively. Her research interest is power system economics and quality analysis.

Shengxiao Dong He received the B.S. degree in electrical engineering from North China Electricity Power University, Beijing, China, in 2016. His main research interest is power system operation.

Gengyin Li He received the B.S., M.S. and Ph. D. degrees, all in Electrical Engineering from North China Electricity Power University in 1984, 1987, and 1996 respectively. His areas of interest include HVDC transmission, and power quality analysis.

Jianwen Ren He received the B.S., M.S. and Ph. D. degrees, all in Electrical Engineering from North China Electricity Power University in 1983, 1987, and 1997 respectively. His areas of interest is power system economics, analysis and reliability.